Layer-by-Layer Growth of Acentric Multilayers of Zr and Azobenzene Bis(phosphonate): Structure, Composition, and Second-Order Nonlinear Optical Properties

Grace A. Neff, Marcus R. Helfrich, Matthew C. Clifton, and Catherine J. Page*

Department of Chemistry and Materials Science Institute, University of Oregon,
Eugene, Oregon 97403

Received August 23, 1999. Revised Manuscript Received May 5, 2000

This paper describes the use of layer-by-layer growth of metal−bis(phosphonate) multilayers to produce acentric thin films with second-order nonlinear optical properties. To incorporate such properties, organic “chromophore” molecules containing conjugated π systems situated between electron donor and electron acceptor groups are oriented uniformly within the film such that the bulk structure is noncentrosymmetric. This is accomplished using chromophoric α,ω-bis(phosphonate) molecules that have one terminal phosphonate group “protected” in ester form, whereas the other is a free phosphonic acid that will bind to a metal-primed silicon or glass surface. After deposition of the acid moiety onto metal-primed silicon, the ester groups are hydrolyzed to enable deposition of additional metal and chromophore layers. We report here the results of this approach using the chromophore bis(1-ethyl)3-{*N*-methyl[(4-[(4-phenylphosphonic acid)azo]phenyl)amino]decyl}phosphonate, or azobenzene molecule **I**. Results from multilayer studies and monolayer and solution studies are discussed, with emphasis on results from UV−vis spectroscopy, grazing angle X-ray diffraction, and second harmonic generation.

Introduction

As current semiconductor technology continues to follow the trend in decreasing circuit dimension proposed by Moore,[1] research in high technology is pushing toward the advancement of the photon as the basis for numerous communications and general circuitry applications. Critical to this advancement is the synthesis of new materials for the basic components of these new devices. Molecule-based materials with large second-order optical nonlinearities are promising candidates in this area, because of their potential application in electrooptic, photorefractive, and second harmonic generation (SHG) devices.[2,3] To attain efficient second-order nonlinear optical (NLO) materials, the constituent molecules in these materials must be organized such that the NLO-active chromophores contained therein are arranged acentrically, as second-order NLO processes are forbidden in centrosymmetric media. Several ingenious techniques exist to align molecules in this manner, including incorporation into Langmuir−Blodgett films and poled polymer films.[4] An alternative approach that has also been shown to be effective at producing such materials is molecular self-assembly.[2,3,5−9]

In recent years, many different systems have been shown to self-assemble into both mono- and multilayer films, and considerable strides have been made in characterizing various aspects of the assembly process as well as the numerous properties of the resulting films. Among the variety of systems studied are the alkyltrichlorosilanes on silicon,[10] disulfides and alkanethiols on gold,[11−15] carboxylic acids on metal oxide surfaces,[16−18] and metal bis(phosphonates)[19−30] and metal diisocyanides[31,32] onto appropriately functional-

---

(1) Mack, C. A. *Opt. Photonics News* **1996**, *7*, 29.
(2) Nie, W. *Adv. Mater.* **1993**, *5*, 520.
(3) Marder, S. R., Sohn, J. E., Stucky, G. D., Eds. *Materials for Nonlinear Optics: Chemical Perspectives*; American Chemical Society: Washington, D. C., 1991; Vol. 455.
(4) Prasad, P. N.; Williams, D. J. *Introduction to Nonlinear Optical Effects in Molecules and Polymers*; Wiley: New York, 1990.
(5) Katz, H. E.; Wilson, W. L.; Scheller, G. *J. Am. Chem. Soc.* **1994**, *116*, 6636.
(6) Katz, H. E.; Scheller, G.; Putvinski, T. M.; Schilling, M. L.; Wilson, W. L.; Chidsey, C. E. D. *Science* **1991**, *254*, 1485.
(7) Lin, W.; Lin, W.; Wong, G. K.; Marks, T. J. *J. Am. Chem. Soc.* **1996**, *118*, 8034.
(8) Li, D.; Ratner, M. A.; Marks, T. J.; Zhang, C.; Yang, J.; Wong, G. K. *J. Am. Chem. Soc.* **1990**, *112*, 7389.
(9) Hanken, D. G.; Naujok, R. R.; Gray, J. M.; Corn, R. M. *Anal. Chem.* **1997**, *69*, 240.
(10) Sagiv, J. *J. Am. Chem. Soc.* **1980**, *102*, 92.
(11) Nuzzo, R. G.; Allara, D. L. *J. Am. Chem. Soc.* **1983**, *105*, 4481.
(12) Nuzzo, R. G.; Fusco, F. A.; Allara, D. L. *J. Am. Chem. Soc.* **1987**, *109*, 2358.
(13) Bain, C. D.; Whitesides, G. M. *J. Am. Chem. Soc.* **1988**, *110*, 3665.
(14) Troughton, E. B.; Bain, C. D.; Whitesides, G. M.; Nuzzo, R. G.; Allara, D. L.; Porter, M. D. *Langmuir* **1988**, *4*, 365.
(15) Bain, C. D.; Biebuyck, H. A.; Whitesides, G. M. *Langmuir* **1989**, *5*, 723.
(16) Allara, D. L.; Nuzzo, R. G. *Langmuir* **1985**, *1*, 45.
(17) Maoz, R.; Sagiv, J. *Langmuir* **1987**, *3*, 1034.
(18) Maoz, R.; Sagiv, J. *Langmuir* **1987**, *3*, 1045.
(19) Lee, H.; Kepley, L. J.; Hong, H.-G.; Mallouk, T. E. *J. Am. Chem. Soc.* **1988**, *110*, 618.
(20) Akhter, S.; Lee, H.; Hong, H.-G.; Mallouk, T. E.; White, J. M. *J. Vac. Sci. Technol., A* **1989**, *7*, 1608.
(21) Cao, G.; Hong, H.-G.; Mallouk, T. E. *Acc. Chem. Res.* **1992**, *25*, 420.
(22) Yang, H. C.; Aoki, K.; Hong, H.-G.; Sackett, D. D.; Arendt, M. F.; Yau, S.-L.; Bell, C. M.; Mallouk, T. E. *J. Am. Chem. Soc.* **1993**, *115*, 11855.
(23) Zeppenfeld, A. C.; Fiddler, S. L.; Ham, W. K.; Klopfenstein, B. J.; Page, C. J. *J. Am. Chem. Soc.* **1994**, *116*, 9158.

10.1021/cm9905444 CCC: $19.00

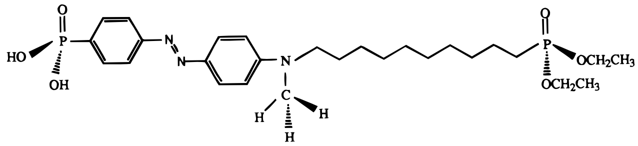

Figure 1. Bis(1-ethyl)3-{*N*-methyl[(4-[(4-phenylphosphonic acid)azo]phenyl)amino]decyl}phosphonate, or azobenzene molecule **I**.

ized oxide or gold surfaces. Use of molecular self-assembly to produce acentric films with second-order NLO properties was first investigated by Marks and coworkers, who studied siloxane-based multilayers with a high degree of structural regularity and resulting high nonlinearity.[7,8] Katz et al. have used molecular self-assembly to produce films of acentric zirconium phosphate/phosphonate multilayers with high second-order optical nonlinearity[5,6] and Hanken et al. have recently reported the use of similar chemistry to produce noncentrosymmetric multilayers with electrooptical properties.[9]

Our approach to incorporating NLO properties into noncentrosymmetric multilayers involves the layer-by-layer growth of acentric metal−bisphosphonate films,[25−27] and is unique in that it involves only phosphonate (P−C) linkages, which are less susceptible to hydrolytic cleavage than are phosphate (P−O−C) linkages.[33] The chemistry used for building multilayers is also fundamentally different; we make use of a bisphosphonate chromophore, bis(1-ethyl)3-{*N*-methyl[(4-[(4-phenylphosphonic acid)azo]phenyl)amino]decyl}phosphonate, azobenzene molecule **I** (Figure 1), which has one terminal phosphonate group "protected" in ester form, whereas the other is a free phosphonic acid that will bind to a metal-primed silicon or glass surface. After deposition of an oriented monolayer of **I** onto a metal-primed surface, acid hydrolysis serves to cleave the ester groups to give a terminal phosphonic acid (note: this process applied to a phosphate linkage would cleave the phosphate from the chromophore, but the phosphonate group remains intact). This enables subsequent deposition of zirconium ions, and repeating this entire process leads to multilayer growth, as shown in Figure 2.

Both mono- and multilayers of **I** and either Hf or Zr were grown on both Si and glass substrates and characterized with a variety of techniques, most notably grazing angle X-ray diffraction (GAXRD), UV−vis spectroscopy, and SHG. The chromophore within molecule **I** has a measurably large second-order hyperpolarizability (vide infra). However, although a large measurable SHG signal is observed for mono- and multilayers, the results described below indicate that the deposition scheme used in these studies compromises the NLO activity of the chromophore during acid hydrolysis. Despite this, multilayers of Zr and **I** on both Si and glass substrates were shown to produce the expected quadratically increasing SH response with increasing number of layers. Further refinements of the deposition scheme are necessary, however, to attain the optimal SH response this system is capable of exhibiting. The SH polarization dependence from multilayers on glass was also examined to determine the average tilt angle of the chromophore portion of the azobenzene molecule **I**.

Experimental Section

Materials. Hafnium oxychloride octahydrate was used as received from Teledyne Wah Chang Albany. Zirconium (IV) acetylacetonate [Zr(acac)$_4$] was used as received from Aldrich. Azobenzene molecule **I** was prepared in a several-step reaction as described below. In all preparations of multilayers and solutions, water deionized to a resistivity of 17−18 MΩ cm with a Barnstead Nanopure II, or 200 proof ethanol, was used.

Substrates, Surface Functionalization, and Layer Growth. The silicon substrates used were Si (100) wafers from Silicon Quest. Wafers were degreased and then functionalized with hafnium as previously described.[23] Glass slides used were precleaned, 75 × 25 mm, 0.96- to 1.06-mm-thick microscope slides from Corning, no. 2947. These were further cleaned by sonicating in aqueous Micro soap solution for 15−30 min, rinsing in flowing Ultrapure water briefly, sonicating for 15−30 min in Ultrapure water, soaking for 5−10 min in each methanol, 1:1 methanol:chloroform, and chloroform, soaking in piranha solution (3:1 H_2SO_4:H_2O_2) (CAUTION: piranha solutions are strongly oxidizing and should be used with extreme care in the absence of organic solvents!) at ~80 °C for 15−30 min, and finally rinsing thoroughly in flowing Ultrapure water for 15−30 min. Glass substrates were functionalized with hafnium metal ions by the same procedure used for the silicon substrates. The mono- and multilayer samples were prepared by immersing a Hf-primed wafer or slide in a 1.25 mM solution of azobenzene molecule **I** in 1:1 ethanol:water at ~55−60° overnight, hydrolyzing in 0.5 M HCl at 45−50 °C overnight, and immersing in either 5 mM aqueous $HfOCl_2$ (pH 2) for 4−5 h or ethanolic Zr[acac]$_4$ (with 2% sodium ethoxide on a mole basis) for 7−8 h. Samples were carefully rinsed between immersion steps with the appropriate solvent.

Synthesis of Azobenzene Molecule I. *Bis(1-ethyl)(10-bromodecyl)phosphonate (**1**)*: A mixture of 40.1 g (0.133 mol) of dibromodecane and 5.48 g (0.0330 mol) of triethyl phosphite were refluxed for 3 h. The mixture was cooled to room temperature and concentrated under vacuum with slight heating for 2 h to remove excess triethyl phosphite. Chromatography on silica gel eluting with hexane to remove the starting material left a fraction that could be stripped from the column with an acetone wash. Removal of the solvent under vacuum gave **1** in 75% yield. ^{1}H NMR in $CDCl_3$: δ 4.065 ppm (m, 4H), δ 3.378 ppm (t, 2H), δ 1.824 ppm (m, 2H), 1.418−1.269 ppm (bm, 22 H). ^{31}P NMR in $CDCl_3$: δ 32.25 ppm (referenced to triphenylphosphine at δ − 18 ppm in $CDCl_3$).

*Bis(1-ethyl)[10-(N-methyl-N-phenylamino)decyl]phosphonate (**2**)*: In a 50-mL three-neck round-bottom flask cooled by ice, an equal mixture of 3 mmol each of *N*-methylaniline and **1** was prepared. To this mixture 0.602 g (7.17 mmol) of $NaHCO_3$ in 6 mL H_2O was added with stirring over a period of 1 h, followed by refluxing overnight. To the reaction mixture 50 mL each of Et_2O and H_2O were added and the Et_2O layer collected. The Et_2O layer was extracted with dilute HBr, the extract neutralized with Na_2CO_3, and the resulting mixture extracted with Et_2O. The product was dried over molecular

---

(24) O'Brien, J. T.; Zeppenfeld, A. C.; Richmond, G. L.; Page, C. J. *Langmuir* **1994**, *10*, 4657.

(25) Neff, G. A.; Page, C. J.; Meintjes, E.; Tsuda, T.; Pilgrim, W.-C.; Roberts, N.; Warren, W. W., Jr. *Langmuir* **1996**, *12*, 238.

(26) Neff, G. A.; Mahon, T. M.; Abshere, T. A.; Page, C. J. *Mater. Res. Soc. Symp. Proc.* **1996**, *435*, 661.

(27) Neff, G. A.; Helfrich, M. R.; Page, C. J. *Phosphorus, Sulfur, and Silicon* **1999**, *53*, 144−146.

(28) Thompson, M. E. *Chem. Mater.* **1994**, *6*, 1168.

(29) Snover, J. L.; Thompson, M. E. *J. Am. Chem. Soc.* **1994**, *116*, 765.

(30) Byrd, H.; Pike, J. K.; Talham, D. R. *Chem. Mater.* **1993**, *5*, 709.

(31) Ansell, M. A.; Cogan, E. B.; Page, C. J. *Langmuir* **2000**, *16*, 1172.

(32) Ansell, M. A.; Cogan, E. B.; Neff, G. A.; von Roeschlaub, R.; Page, C. J. *Supramol. Sci.* **1997**, *4*, 21.

(33) Vide infra: a phosphate ester linkage would be cleaved by the conditions we use to hydrolyze the phosphonate ester in step 2 of our synthetic scheme.

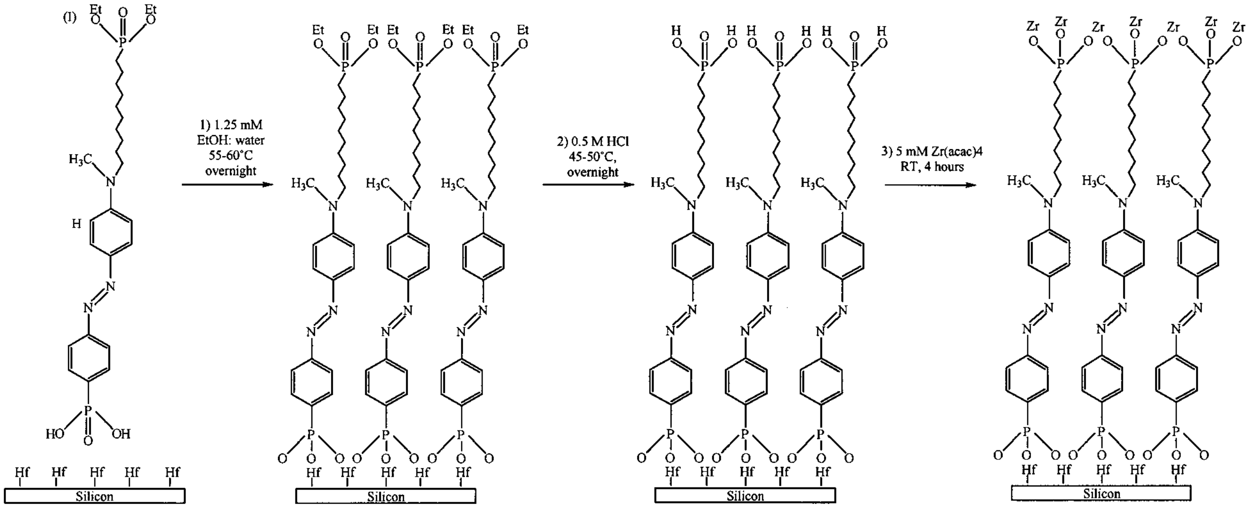

Figure 2. Scheme for producing acentric multilayers with **I** and zirconium ions.

sieves, filtered, and concentrated to give 0.450 g (1.17 mmol) of the pure product (**2**) for further use (38.5% yield). ^{1}H NMR in $CDCl_3$: δ 7.273−7.201 ppm (m, 3H), δ 6.714−6.652 ppm (m, 2H), δ 4.139−4.058 ppm (m, 4H), δ 3.30 ppm (t, 2H), δ 2.928 ppm (s, 3H), δ 1.784−1.288 ppm (m, 18H). ^{31}P NMR in $CDCl_3$: δ 32.736 ppm (referenced to TPP at δ −18 ppm in $CDCl_3$).

*Bis(1-ethyl)3-{N-methyl-[(4-[(4-phenylphosphonic acid)azo]-phenyl)amino]decyl}phosphonate (**3**)*: In a 50-mL round-bottom flask cooled to 0 °C, a solution of 0.043 g (0.623 mmol) sodium nitrite in 2 mL of deionized H_2O was added dropwise to a solution of 0.102 g (0.589 mmol) of 4-aminophenylphosphonic acid dissolved in 5 mL of 6 M HCl. The reaction was allowed to stir for 15 min, after which 0.221 g (0.575 mmol) of product (**2**) was dissolved in the minimum amount of EtOH and was added slowly to the stirring reaction mixture. The reaction went red instantaneously with the addition of the substituted phosphonate ester. The reaction was allowed to stir at 0 °C for 2 h. After this, 0.163 g (1.20 mmol) of solid sodium acetate was added to the reaction while stirring and the reaction was allowed to come to room temperature slowly. The product was extracted with diethyl ether, leaving **3** in the aqueous layer. The H_2O was removed under reduced pressure to yield a red gumlike solid. The solid was taken up in methanol, dried using sodium sulfate, then removed under vacuum leaving a red solid (**3**) (55% yield; overall yield 16%). ^{1}H NMR in CD_3OD: δ 1.3 ppm (m, 24 H), δ 3.2 ppm (s, 3H), δ 3.55 ppm (m, 2H), δ 4.0 ppm (m, 4H), δ 6.8 ppm (m, 2H), δ 7.5 ppm (m, 2H), δ 7.6 ppm (m, 2H), δ 7.8 ppm (m, 2H). ^{31}P NMR in CD_3OD: δ 34.085 ppm and δ 15.011 ppm. Mass spectrum *m*/*e*: 570.7 (M^+). IR: 3396 cm^{-1} (w), 3058 cm^{-1} (m), 2983 cm^{-1} (s), 2929 cm^{-1} (s), 2856 cm^{-1} (s), 2674 cm^{-1} (wb), 1600 cm^{-1} (m), 1496−1450 cm^{-1} (m), 1429 cm^{-1} (w), 1390 cm^{-1} (m), 1197 cm^{-1} (s), 1133 cm^{-1} (s), 1024 cm^{-1} (m).

Physical Characterization. The azobenzene molecule **I** was characterized after synthesis using ^{1}H and ^{13}C NMR, and IR and UV−vis spectroscopies. It was also characterized by NMR before and after subjection to the deprotection conditions used in layer growth. NMR samples were run in deuterated methanol using a Varian Inova-300 NMR instrument.

Optical ellipsometry (at 632.8 nm) and GAXRD measurements were performed as previously described.[23,26,27] During the time that this study was conducted, the ellipsometer alignment was suspect, and ellipsometry data is thus only used as a qualitative verification of film growth.

UV−Vis spectra were acquired on a Perkin-Elmer Lambda 6 UV−vis spectrometer with PECSS system software. Spectra in solution were typically run against an ethanol reference after a background correction was run on ethanol in both cells, from 200 to 600 nm at 60 nm/min. Spectra from films on glass slides were run against a reference of a Hf-primed glass slide after background correction on clean glass slides. Spectra were obtained in the 250 to 700 nm range at 20 nm/min. Spectra in both cases were used qualitatively to identify differences between the protonated and nonprotonated forms of the azobenzene molecule **I**; these differences were used to follow and interpret data collected after successive steps in the multilayer deposition process. Spectra from glass slides were also used to quantify the amount of chromophore deposited in each azobenzene deposition step. This was determined by integrating the area under the peak centered at ∼430 nm.

SHG measurements were performed using the 800-nm output of a regeneratively amplified Ti:sapphire laser operating at 1 kHz. The laser light was collimated to a beam diameter of ∼3 mm. Approximately 80% of this was directed onto the sample at a 45° angle of incidence. The SH signal at 400 nm was collected in reflection by a monochromator, photomultiplier tube, and gated electronics for a period of 5 min to ensure that the signal was stable. The remaining 20% of the laser light was passed through a 200-μm-thick type I phase-matched potassium dihydrogen phosphate (KDP) crystal to provide a reference SH signal. The signal from the multilayers was normalized to this reference signal from KDP. Polarization dependence of the SH signal was also investigated, by inclusion of a waveplate in the beam path before the sample and a polarizer after the sample.

Results

Multilayer studies. Multilayer samples prepared using azobenzene molecule **I** and $Zr(acac)_4$ solutions on both silicon and glass substrates were studied using a variety of characterization techniques. A multilayer sample was prepared on the same Hf-primed silicon substrate, with successive pieces of this substrate cut from the larger whole after deposition of a certain number of layers was accomplished. Five samples resulted, with 2, 4, 6, 7, and 8 layers, respectively. Each sample was individually characterized using ellipsometry and GAXRD as it was cut from the larger whole, and several different areas on the remaining whole piece were also characterized by ellipsometry and GAXRD after each successive layer. Ellipsometry data was used to qualitatively monitor film growth, and indicated that each layer was uniform across the sample and that growth was uniform. Accurate film thicknesses were determined by analyzing the fringes observed in the GAXRD data (using a modified Bragg equation, as discussed elsewhere[23]). The total film thickness determined by this technique is shown as a function of

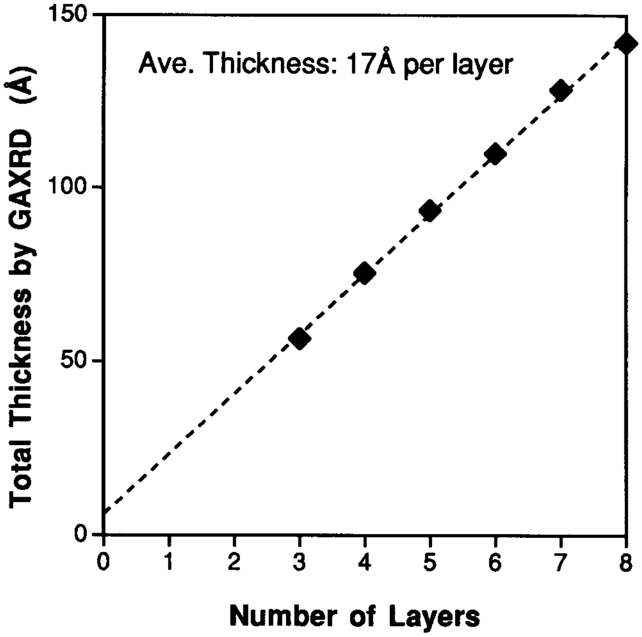

Figure 3. Total film thickness from GAXRD data as a function of the number of layers of **I** and Zr on a Hf-primed silicon substrate. Error bars are on the order of the symbol size in the plot.

number of layers in Figure 3. The slope of these data gives the thickness per layer of 17.3 Å, which indicates that these films are thinner than would be expected from the modeled length of the fully extended azobenzene molecule **I** (~29 Å/layer). This implies that the layers are tilting significantly from the surface normal. Some tilting is expected because tilt angles for self-assembled alkyl chain-containing monolayers are commonly ~30°, and the azobenzene moiety requires a packing motif with more space between adjacent bisphosphonates than required by alkyl bisphosphonates, as discussed later. The thickness observed is consistent with an overall tilt angle of the molecules of ~54° from the surface normal. It is possible that the rigid chromophore portion and the alkyl chain portion of the molecules have different tilt angles. This cannot be determined from ellipsometry or GAXRD data; however, SH polarization studies discussed later do indicate a slightly larger tilt angle for the chromophore portion of the molecule.

The second harmonic (SH) response was measured for each of the five multilayer samples grown on Si. The square root of the SH intensity as a function of number of layers is shown in Figure 4. These samples exhibit a quadratic increase in SH response with increasing number of layers, which is expected for multilayers composed of individual layers of uniform thickness and chromophore orientation.

To establish that the observed SH response is attributable to the incorporation of oriented chromophores and not due to the zirconium phosphonate layers, we also investigated the SH response of zirconium–decylbis(phosphonic acid) multilayers grown on a hafnium-functionalized silicon substrate. The SH response was measured as a function of the number of layers, after zirconium deposition. There was no measurable difference in the response of these films compared with the metal-primed substrate.

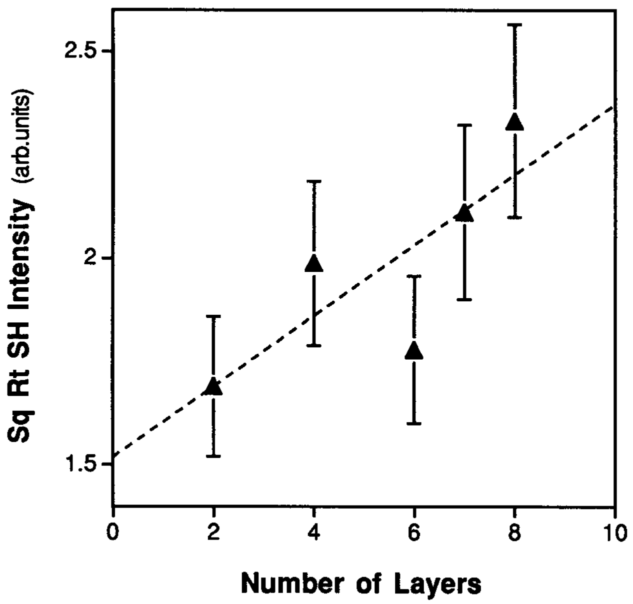

Figure 4. Square root of the SH intensity as a function of the number of layers of **I** and Zr on a Hf-primed silicon substrate.

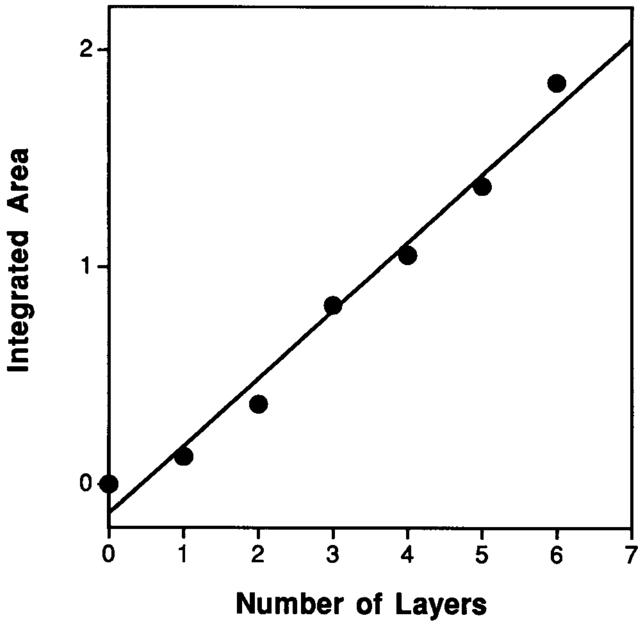

Figure 5. Integrated area under the major absorbance peak (425 nm) as a function of the number of layers of **I** and Zr on Hf-primed glass.

Multilayer samples were also prepared on glass slides, and characterized with UV–vis spectroscopy and SHG. Four different pieces of glass slides served as substrates for the four multilayer samples that were grown simultaneously, and characterization data from each are combined to compose the plots described below. UV–vis spectroscopy was used to follow the deposition, and to verify that roughly the same amount of chromophore was deposited in each azobenzene deposition step. Figure 5 shows the integrated intensity of the 425-nm peak as a function of number of layers. This peak is associated with the π–π^* transition of the nonprotonated form of the azobenzene molecule **I**. This plot indicates that roughly the same amount of chromophore is deposited in each deposition cycle. The SH response

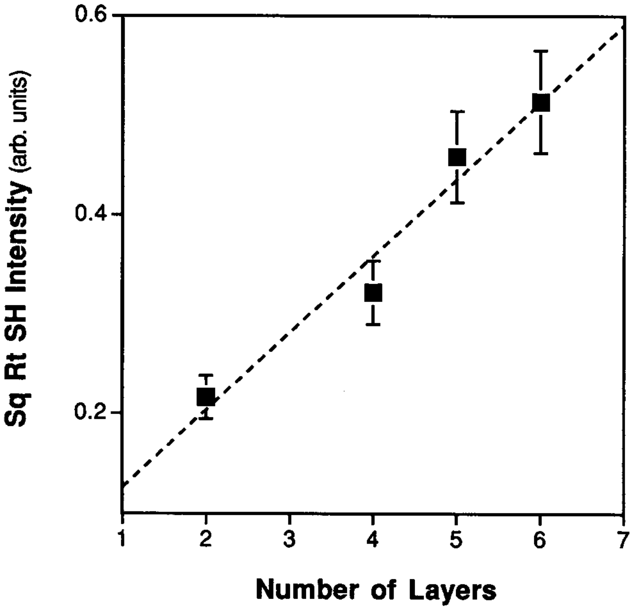

Figure 6. Square root of the SH intensity as a function of the number of layers of **I** and Zr on Hf-primed glass.

from these films is shown in Figure 6, which shows the expected linear increase in the square root of the SH response with increasing number of layers. A comparison with the SH response of identical films grown on silicon substrates indicates that multilayer samples of approximately the same quality can be obtained on either substrate.

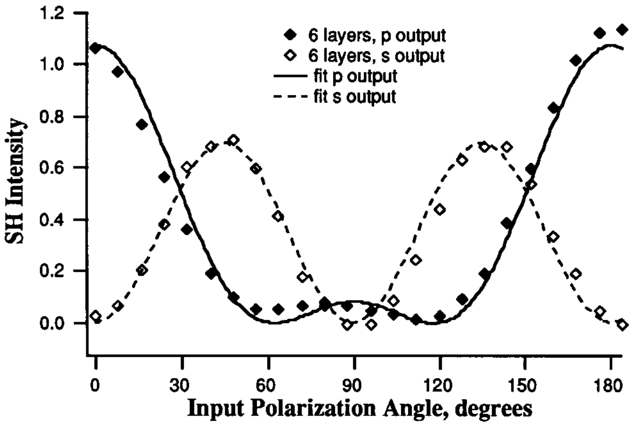

Figure 7. SH Intensity as function of input polarization angle for six layers of **I** and Zr on Hf-primed glass substrates. Lines are fits to the data as discussed in the text.

Further characterization of the structure of the films on glass was accomplished through SH polarization dependence studies. Studies of this nature can yield orientational information, in the form of an average tilt angle relative to surface normal for the chromophore portion of the NLO-active molecule.[34,35] This has been previously demonstrated by several groups.[36−42] In the work here, the basic phenomenological method and assumptions used by Corn's group to study methylene blue orientation on Pt and Si surfaces[34,35] are followed. Accordingly, the polarization angle of the incoming laser light impinging on the samples was varied from 0 to 180° through use of a waveplate, and the output polarization was controlled with a polarizer placed after the sample. The SH response as a function of input polarization angle was measured for both p and s output polarization. The data obtained in this manner for six layers of azobenzene molecule **I** and Zr on Hf-primed glass is shown below in Figure 7. In this plot, 0° corresponds to p input polarization and 90° corresponds to s input polarization. To determine the average molecular orientation, we assume that the molecules have an orientational distribution function that is invariant upon rotation about the surface normal (i.e., the molecules have no preferred direction in the plane) and that they have a plane of symmetry. In this case, only three tensor components contribute to $\chi^{(2)}$, namely, $\chi^{(2)}{}_{ZZZ}$, $\chi^{(2)}{}_{ZXX}$, and $\chi^{(2)}{}_{XXZ}$. These components contribute to the observed response according to the following equations:[34]

$$I_s \propto |a_1 \sin 2\gamma\, \chi^{(2)}{}_{XXZ}|^2 \qquad (1)$$

$$I_p\,(2\omega) \propto |[a_2\chi^{(2)}{}_{XXZ} + a_3\chi^{(2)}{}_{ZXX} + a_4\chi^{(2)}{}_{ZZZ}]\cos^2\gamma + (a_5\chi^{(2)}{}_{ZXX})\sin^2\gamma|^2 \qquad (2)$$

where γ is the polarization angle of the incident light ($\gamma = 0°$ for p-polarized light and $\gamma = 90°$ for s-polarized light) and the a_i terms are products of the components of $e_i(\omega)$ and $e_i(2\omega)$ terms, which are the components of the vectors for the fundamental and SH wavelengths, and are derived from the appropriate Fresnel factors.[34,35] These calculations were simplified by considering only the front face of the glass slide, and so the angle of incidence and the angle at which the SH is generated are both 45°. As a result of this simplification there is only one interface to consider, that of air to glass. Fresnel coefficients were appropriately calculated for this interface at 45° using the expressions found in Fowles.[43] The $\chi^{(2)}$ elements were determined for these data by calculating the a_i terms and then fitting the appropriate data from 0° to 180° input polarization to expressions (1) and (2) using Igor Pro. The fits are shown in Figure 7. From the fits for the p output data, the $\chi^{(2)}{}_{IJK}$ values were obtained and then used to calculate a ratio of β_{ijk} elements according to the expression:[35]

$$\beta_r = \beta_{xxz}/\beta_{zxx} = [\chi^{(2)}{}_{ZZZ} + 2\chi^{(2)}{}_{XXZ}]/[\chi^{(2)}{}_{ZZZ} + 2\chi^{(2)}{}_{ZXX}] \qquad (3)$$

This ratio is then used along with the $\chi^{(2)}{}_{IJK}$ values to determine the angle ζ using expression (4).[35] The angle ζ is defined as the average angle between the

---

(34) Campbell, D. J.; Higgins, D. A.; Corn, R. M. *J. Phys. Chem.* **1990**, *94*, 3681.

(35) Higgins, D. A.; Byerly, S. K.; Abrams, M. B.; Corn, R. M. *J. Phys. Chem.* **1991**, *95*, 6984.

(36) Heinz, T. F.; Chen, C. K.; Ricard, D.; Shen, Y. R. *Phys. Rev. Lett.* **1982**, *48*, 478.

(37) Heinz, T. F.; Tom, H. W. K.; Shen, Y. R. *Phys. Rev. A* **1983**, *28*, 1883.

(38) Rasing, T.; Shen, Y. R.; Kim, M. W.; Valint, P.; Bock, J. *Phys. Rev. A* **1985**, *31*, 537.

(39) Rasing, T.; Shen, Y. R.; Kim, M. W.; Grubb, S.; Bock, J. *Phys. Rev. Lett.* **1985**, *55*, 2903.

(40) Hicks, J. M.; Kemnitz, K.; Eisenthal, K. B.; Heinz, T. F. *J. Phys. Chem.* **1986**, *90*, 560.

(41) Kemnitz, K.; Bhattacharyya, K.; Hicks, J. M.; Pinto, G. R.; Eisenthal, K. B.; Heinz, T. F. *Chem. Phys. Lett.* **1986**, *131*, 285.

(42) Smiley, B. L.; Vogel, V. *J. Chem. Phys.* **1995**, *103*, 3140.

(43) Fowles, G. R., Ed. *Introduction to Modern Optics*, 2nd ed.; Dover Publications: New York, 1975.

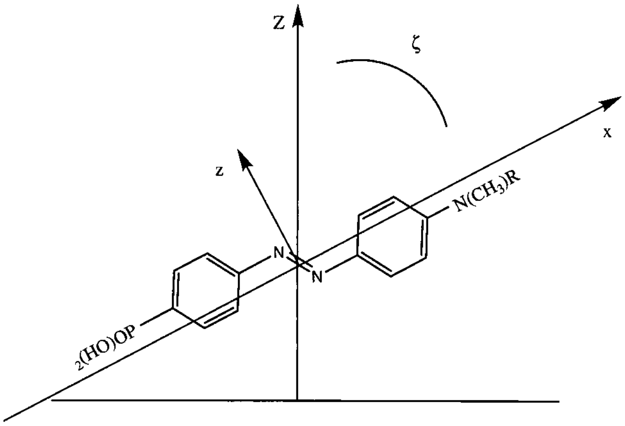

Figure 8. Relation between molecular axes *x*, *y*, and *z* and surface axes *X*, *Y*, and *Z* for the chromophore, and the definition of angle ζ, defined as the average angle between the transition dipole moment and the surface normal.

transition dipole moment and the surface normal, as illustrated in Figure 8. For the azobenzene **I**, the dipole transition is assumed to be along the long axis of the chromophore portion of the molecule.

$$\cos^2 \zeta = (1 + 2\beta_r)^{-1}[\chi^{(2)}{}_{ZZZ}]/[\chi^{(2)}{}_{ZZZ} + 2\chi^{(2)}{}_{ZXX}] \quad (4)$$

The β ratio for the six-layer film was found to be 1.82 by this analysis, corresponding to an average chromophore tilt angle of ~62° from the surface normal. This is slightly higher than the 54° tilt angle suggested by GAXRD thicknesses (Figure 3). This suggests that the hydrocarbon chains of the molecules are tilted slightly less with respect to surface normal compared with the chromophore portion. Overall, the large tilt angle of the chromophore suggests that there is significant distance between binding sites of adjacent azobenzene molecules; this could be a result of the large girth of the azobenzene moiety relative to the metal–phosphonate network.

Protonation: Solution Studies. Although the expected quadratic increase in SH response was observed with increasing numbers of chromophore in multilayers grown on glass and silicon, we wanted to assess the impact of the hydrolysis step on the chromophore activity, because the NLO activity of the chromophore used in this study could be adversely affected by protonation. To establish whether protonation of the chromophore in the film was a problem, we first studied ethanolic solutions of **I** using UV–vis spectroscopy. Figure 9 shows the spectra for a ~0.2 mM solution of **I** as synthesized (dashed trace) and a ~0.1 mM solution of the same species after being brought to pH 1 with HCl and heating to ~60 °C overnight (solid trace). Clearly the chromophore species is altered upon subjection to hydrolysis conditions. This can also be seen visually; ethanolic solutions of **I** as-synthesized are bright yellow, whereas those of the species after acid treatment are bright pink. This behavior is similar to that observed for the acid/base indicator methyl orange, which is yellow above pH 3.4 (basic form) and pink below pH 2 (acidic form).[44] Methyl orange is an azo dye with a structure similar to **I**. The color change observed for **I** is a consequence of an observed shift in the dominant absorbance band from ~425 nm (basic form) to ~517 nm (acidic form) upon protonation of the chromophore. The clear difference in absorbance spectra for the two species was used to follow the degree of protonation of the chromophore during the multilayer deposition process, as described below.

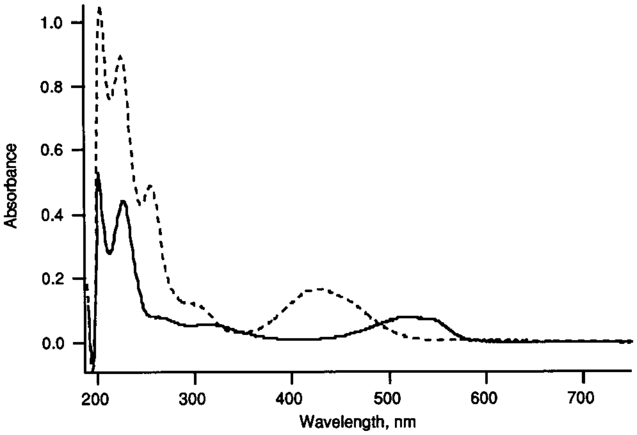

Figure 9. UV–vis spectra of ethanol solutions of azobenzene molecule **I** before (broken trace) and after (solid trace) subjection to acid hydrolysis conditions.

Protonation: Mono- and Multilayer Studies. To study the effects of hydrolysis on the chromophore after incorporation into a film, a series of studies involving UV–vis spectroscopy and SHG were conducted on mono- and multilayer samples of **I** and Zr(acac)$_4$ grown on glass. To determine the effects of the protonation on the NLO properties of the films, the SH response of similar films after each step in the deposition cycle was examined. UV–vis spectra of monolayers and multilayers before hydrolysis, after hydrolysis, and after Zr(acac)$_4$ treatment echoed the solution-phase studies. A shift from ~430 nm to ~510 nm in the absorption band upon hydrolysis (protonation) was observed that was essentially restored to the deprotonated absorption band (~430 nm) after Zr(acac)$_4$ treatment. Figure 10 shows the SH response from four different monolayer samples of **I** on Hf-primed glass slides before and after acid hydrolysis and after Zr deposition. In the last step, samples 1 and 2 were soaked in ethanolic Zr[acac]$_4$ with no added base, whereas samples 3 and 4 were soaked in ethanolic Zr[acac]$_4$ with 2 mol % sodium ethoxide. The signal before hydrolysis was easily measurable, and significantly larger than that from the metal-primed substrate. However, the SH response decreased by ~50% upon acid hydrolysis, suggesting protonation of functional groups within the NLO-active chromophore. Protonation of the amine or the azo functionality of **I** would serve to lower the second-order NLO response of this molecule: protonation of the amine would lessen its donor capabilities, whereas protonation of the azo group would disrupt the conjugation within the chromophore. Interestingly, upon capping with Zr, the SH signal is not restored to the original intensity observed before to hydrolysis, even though the UV–vis studies suggest that exposure to Zr(acac)$_4$ both with and without added base deprotonates **I** to a high degree. This suggests that protonation alone cannot account for the observed decrease in the SH response.

---

(44) Kemp, D. S.; Vellaccio, F. *Organic Chemistry*; Worth Publishers: New York, 1980.

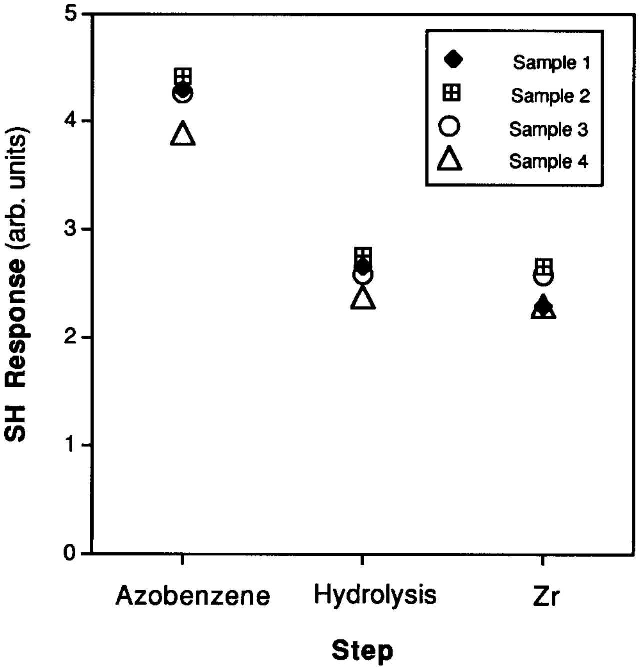

Figure 10. SH response of four different monolayers of **I** as-deposited on a Hf-primed substrate, after hydrolysis, and after Zr deposition.

To rule out the possibility that chromophore is removed from the monolayer during hydrolysis, we used ellipsometry to study several samples of **I** grown on Hf-primed silicon. In all cases there was no change in the thickness of the monolayer upon hydrolysis, so the decrease in SH response upon hydrolysis cannot be explained by loss of chromophore from the monolayer.

One possible explanation is that structural disorder is introduced in the film upon acid hydrolysis and that this order cannot be reestablished upon deprotonation because the disordered orientation of the chromophore molecules is trapped upon capping with zirconium ions. To test whether the Zr deposition “traps” disorder in the chromophore layer, experiments were designed to separate the effect of the metal capping from the effect of deprotonation. Thus, three different film samples with a hydrolyzed layer of **I** were exposed to solutions of acetylacetonate, 10^{-4} M sodium ethoxide in ethanol, and acetylacetonate buffer (in order of increasing basicity—a pH meter measured ~6, 7, and 8, respectively). The resulting SH response after each successive treatment is shown in Figure 11. None of the treatments restored the SH response to the original level observed before hydrolysis. The effect of two of the three treatments was also examined using UV–vis spectroscopy (the sodium ethoxide solution and the acac buffer), and both appear to deprotonate the chromophore. These results demonstrate that the change in SH response upon acid hydrolysis cannot be corrected by simply deprotonating the chromophore, and suggests that the change in the chromophore layer upon hydrolysis is structural as well as chemical.

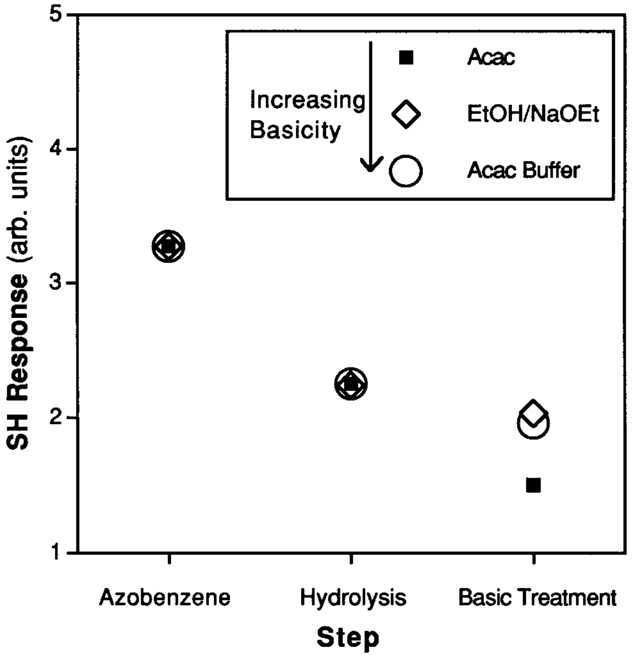

Figure 11. SH response from three different azobenzene **I** monolayer samples, as-deposited on a Hf-primed substrate, after hydrolysis, and after deprotonation by treatment with three different solutions.

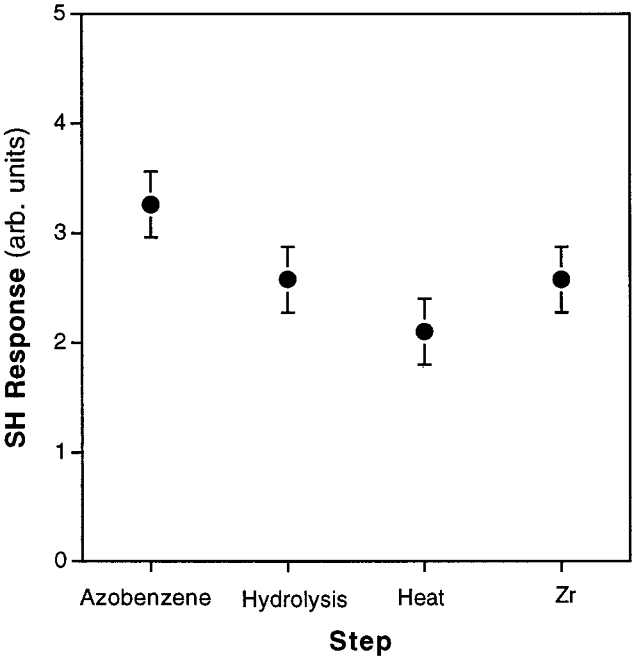

Figure 12. SH response of a monolayer of azobenzene I, as-deposited, after hydrolysis, after a subsequent heat treatment, and after Zr deposition.

A final study conducted on a hydrolyzed chromophore monolayer was a simple heat treatment (60 °C) in ethanol overnight to determine whether “annealing” the films could restore the SH response. The result is shown in Figure 12. Clearly, such heating does not increase the SH response of the film; to the contrary, heating appears to decrease the SH response. Interestingly, the thermally induced decrease is apparently corrected by subsequent capping with the metal layer.

The cause of the observed decrease in SH response upon acid hydrolysis and the inability to restore the SH response of the chromophore by deprotonation remains a mystery. A structural change to the chromophore could result from isomerization of the azobenzene moiety (trans–cis), although there is no evidence in the literature that protonation (most likely of the amine functionality) induces isomerization. Reversible photoisomerization is a well-known phenomenon with stilbene and azobenzene molecules. For example, Matsumoto et al. have reported the trans–cis photoisomerization of an azobenzene derivative in a Langmuir–Blodgett film by excitation with light at 365 nm and reversal at 436 nm. They observed a morphological change from smooth films to puckered films upon photoisomerization from the trans to the cis form,[45] affirming that packing of the cis form is much less efficient. Sato et al. have reported the trans–cis photoisomerization of an azobenzene derivative in a Langmuir–Blodgett film by excitation with light at 356 nm and reversal at 440 nm. They observed the SH produced in such films with the 1064-nm output of a Nd:YAG laser to decrease upon irradiation by UV light (which promotes formation of the cis isomer) and increase after irradiation with visible light (which promotes the trans form).[46]

In the case of a self-assembled film, where the film is covalently bound to a substrate, puckering cannot occur. Wolf and Fox have shown that cis stilbene-containing molecules self-assembled on a gold surface can be photoisomerized to the trans form, but that trans azo molecules self-assembled on a surface cannot be photoisomerized to the cis form, presumably because of steric considerations.[47] In the self-assembled films reported here, the mismatch between the azobenzene molecular girth and the underlying metal ion layer may be significant, leading to an inefficiently packed film. Generally, metal bisphosphonate films are assumed to adopt a structure similar to that of α-$ZrPO_4 \cdot H_2O$.[48] This structure can accommodate various functional groups within bisphosphonate molecules with a cross-sectional area of 24 Å^2 or less, or a van der Waals diameter of approximately 5.3 Å.[49] However, the azobenzene moiety used here has a van der Waals diameter of 7.2 Å,[50] suggesting that this molecule may be too bulky to form an efficiently packed film. Accordingly, there may be sufficient void space in the layers of the azobenzene bisphosphonate layers to allow for trans–cis isomerization. However, photoisomerization at either of these wavelengths was not explicitly carried out in our experiments, and the SH light (400 nm) produced by the films should not promote isomerization in either direction (this falls near the isosbestic point in the cis and trans absorption spectra). If such an isomerization is occurring simply upon protonation, it is without precedent.

In the case of the stilbene-containing molecules incorporated into self-assembled films on gold, a photodimerization reaction also occurred.[47] This type of 2+2 addition is not possible in the azobenzene **I** used in this study. However, a tautomerization could occur upon protonation that ultimately could lead to hydrolysis and cleavage of the alkylamine from azobenzene **I**.[51] This possibility is unlikely because ellipsometry shows no change in film thickness upon hydrolysis. Furthermore, regular multilayer growth is observed. If tautomerization followed by hydrolysis of the azobenzene–amine bond was responsible for the ~50% decrease in SH activity, then one might expect ~50% of the azobenzene **I** molecules to have dissociated to lose the aminodecylphosphonic acid chain, in which case regular multilayer growth would not occur.

Whatever the cause of the reduced SH response induced by hydrolysis, it is important to note that quadratic increases are observed in the SH intensity as a function of number of layers. This implies that the (reduced) activity in each layer is uniform, and also that if this reduction in SH activity can be prevented or reversed, the overall activity per layer would be essentially doubled, and that of the film as a whole would be enhanced quadratically as a function of the number of layers from that observed currently.

Summary and Conclusions

The method reported here of preparing polar multilayers of metal–bis(phosphonates) via layer-by-layer growth has proven to be viable. Our particular method involves use of acentric bis(phosphonate) molecules, protected at one terminus by a phosphonate ester group with a free phosphonic acid group on the other end that can bind to Hf-primed SiO_2 surfaces. Gentle acid hydrolysis of the ester groups in 0.5 M HCl and subsequent metal binding allows for the process to be repeated to build multilayers. This method has successfully been used with the azobenzene molecule **I** and zirconium acetylacetonate solutions to produce regular multilayers on both Si and glass substrates that have been characterized with ellipsometry, GAXRD, UV–vis spectroscopy, and SHG.

Ellipsometry and GAXRD show consistent growth of multiple layers for samples of **I** and Hf or Zr grown on silicon or glass substrates. GAXRD of films grown on Si substrates consistently indicated layer thicknesses of ~17–18 Å/layer for several samples studied, suggesting that the layers tilt significantly from the surface normal. UV–vis spectroscopy of both solutions and films of **I** allowed an assessment of the protonation incurred over the course of the three-step deposition scheme used here. This technique verified protonation of the azobenzene chromophore portion of the molecule during acid hydrolysis and indicated nearly complete deprotonation of the same groups after deposition of the zirconium ions from a $Zr(acac)_4$ solution. SHG studies on monolayer films showed a decrease in the SH response from hydrolyzed monolayers relative to the signal observed from monolayers of azobenzene molecule **I** as deposited, which is at least partially attributed to protonation of the chromophore. However, the SH response was not restored upon deprotonation and deposition of Zr ions using a neutral solution of $Zr[acac]_4$.

Multilayer films were also deposited on glass substrates, with regular layer growth evidenced by UV–vis spectroscopy, which showed roughly the same amount of chromophore deposited in each cycle of azobenzene

---

(45) Matsumato, M.; Miyazaki, D.; Tanaka, M.; Azumi, R.; Manda, E.; Kondo, Y.; Yoshino, N.; Tachibana, H. *J. Am. Chem. Soc.* **1998**, *120*, 1479.

(46) Sato, O.; Baba, R.; Hashimoto, K.; Fujishima, A. *Denki Kagaku oyobi Kogyo Butsuri Kagaku* **1994**, *62*, 530.

(47) Wolf, M. O.; Fox, M. A. *J. Am. Chem. Soc.* **1995**, *117*, 1845.

(48) Clearfield, A.; Smith, G. D. *Inorg. Chem.* **1969**, *8*, 431.

(49) Alberti, G.; Costantino, U.; Marmottini, F.; Vivani, R.; Zappelli, P. *Angew. Chem., Intl. Ed. Eng.* **1993**, *32*, 1357.

(50) Wolf, H.; Ringsdorf, H.; Delamarche, E.; Takami, T.; Kang, H.; Michel, B.; Gerber, C.; Jaschke, M.; Butt, H.-J.; Bamberg, E. *J. Phys. Chem.* **1995**, *99*, 7102.

(51) Smith, P. A. S. *Derivatives of Hydrazine and Other Hydronitrogens Having N–N Bonds*; Benjamin/Cummings: Reading, MA, 1983; p. 176.

deposition. The expected quadratic SH response as a function of number of layers was also seen for films grown on glass. The structure of these films was further characterized via SH polarization dependence studies, which determined the average tilt angle for the chromophore portion of **I** to be ∼62°. Such a significant tilt angle is consistent with the thickness determined by GAXRD.

Further studies are underway to examine the cause of the irreversible reduction in SH response of the chromophore after the hydrolysis step. To test whether trans−cis isomerization is occurring, hydrolyzed films will be photolyzed with visible light to restore an all-trans configuration. In situ SHG studies are planned to help determine the origin of this decrease, as well as to determine ways to reverse this decrease and in general optimize film growth and properties. Atomic force microscopy studies will also be used to examine whether topological changes occur upon hydrolysis. Other chromophore systems that do not have the potential for isomerization are also under consideration for use in this approach.

Acknowledgment. NSF (CHE-9633062 and CHE-9978556) is gratefully acknowledged for support of this research. We also acknowledge support for M.C.C. through the University of Oregon Chemical Physics Institute NSF-REU program (CHE-9531402). We thank Professor G. L. Richmond and Dr. Derek Gragson for allowing us the use of their laser equipment and for help with the experimental setup for measuring SHG. We thank Elizabeth Hommel and Meng Ouyang for the SHG measurements of the zirconium decylbis(phosphonic acid) films.

CM9905444